Fluorescence Indicator Displacement Detection Based on Pillar[5]arene-Assisted Dye Deprotonation

Bin Hua, Li Shao, Guocan Yu and Feihe Huang*

State Key Laboratory of Chemical Engineering, Center for Chemistry of High-Performance & Novel Materials, Department of Chemistry, Zhejiang University, Hangzhou 310027, P. R. China

Fax and Tel: +86-571-8795-3189; Email: fhuang@zju.edu.cn

Electronic Supplementary Information

1. Materials and methods

All reagents were commercially available and used as supplied without further purification. Solvents were either employed as purchased or dried according to procedures described in the literature. Compounds **AP5** and **1** were synthesized according to previous literature.[S1] NMR spectra were recorded with a Bruker Avance DMX 400 spectrophotometer or a Bruker Avance DMX 500 spectrophotometer with the deuterated solvent as the lock and the residual solvent or TMS as the internal reference. The ITC experiments were performed on a VP-ITC micro-calorimeter (Microcal, USA). The fluorescence experiments were conducted on an RF-5301 spectrofluorophotometer (Shimadzu Corporation, Japan). UV-vis spectra were taken on a Shimadzu UV-2550 UV-vis spectrophotometer. Low-resolution electrospray ionization (LRESI) mass spectra were obtained on a Bruker Esquire 3000 plus mass spectrometer (Bruker-Franzen Analytik GmbH Bremen, Germany) equipped with an ESI interface and an ion trap analyzer. High-resolution mass spectra (HRMS) were obtained on a WATERS GCT Premier mass spectrometer. The melting points were collected on a SHPSIC WRS-2 automatic melting point apparatus.

*2. Synthesis of the monomer **M***

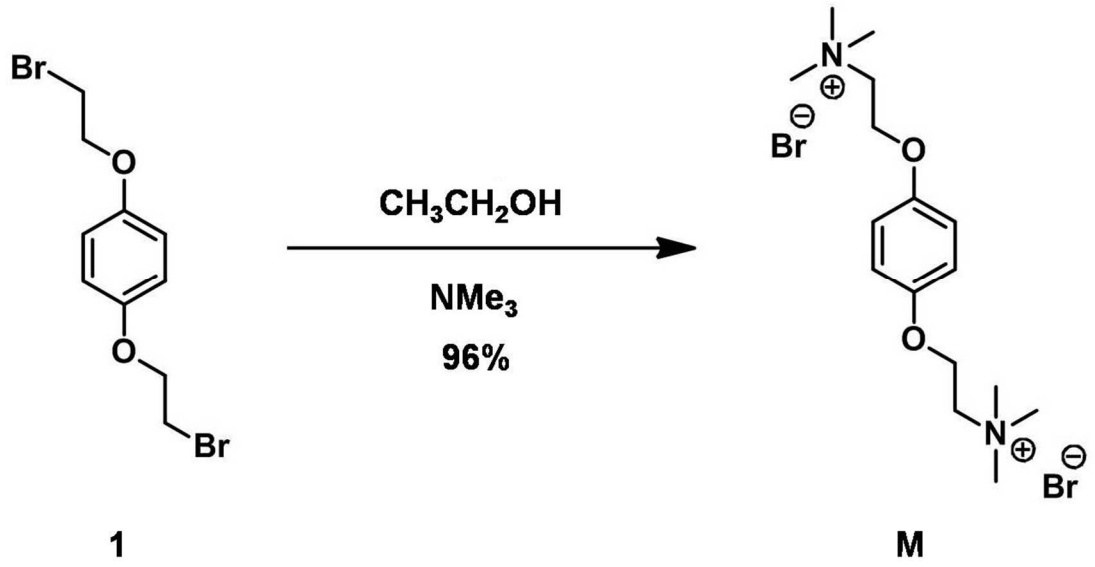

Scheme S1. Synthesis of **M**

Trimethylamine (33% in ethanol, 5.00 mL) and compound **1** (324 mg, 1.00 mmol) were added to ethanol (50 mL), and the solution was refluxed for 12 h. The solvents and excess trimethylamine were evaporated under vacuum. The resulting precipitate was filtered and dried to afford product **M** as a white solid (424 mg, 96%), mp: 304.0−305.8 ºC. The ^{1}H NMR spectrum of **M** is shown in Figure S1. ^{1}H NMR (400 MHz, D_2O, 298 K) δ (ppm): 6.91 (s, 4H), 4.36 (t, J = 2 Hz, 4H), 3.68 (t, J = 4 Hz, 4H), 3.13 (s, 18H). The ^{13}C NMR spectrum of **M** is shown in Figure S2. ^{13}C NMR (100 MHz, D_2O, 298 K) δ (ppm): 154.72, 118.78, 67.85, 65.22, 56.73. LRESIMS is shown in Figure S3: *m/z* 141.3 $[M - 2Br]^{2+}$; *m/z* calcd for $[M - 2Br]^{2+}$ $C_{16}H_{30}N_2O_2^{2+}$, 141.1148; found 141.1144, error − 3 ppm.

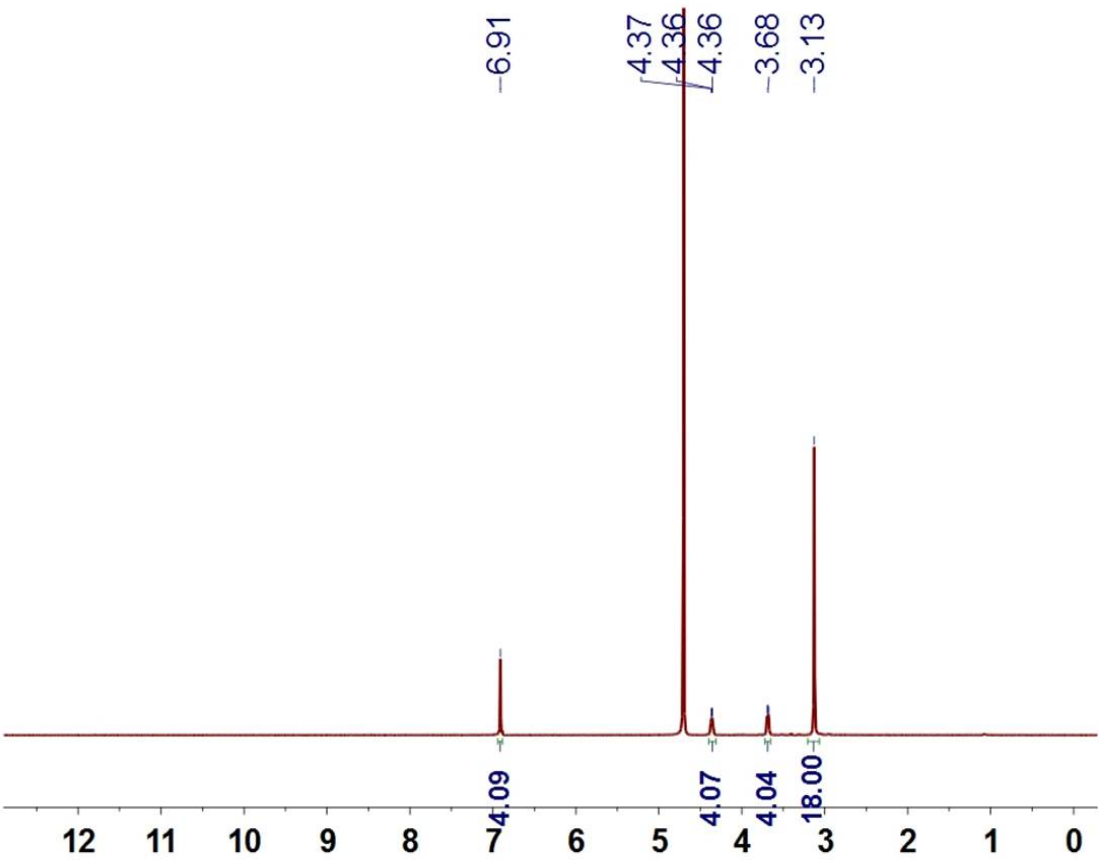

Fig. S1 ^{1}H NMR spectrum (400 MHz, D_2O, 293 K) of **M**.

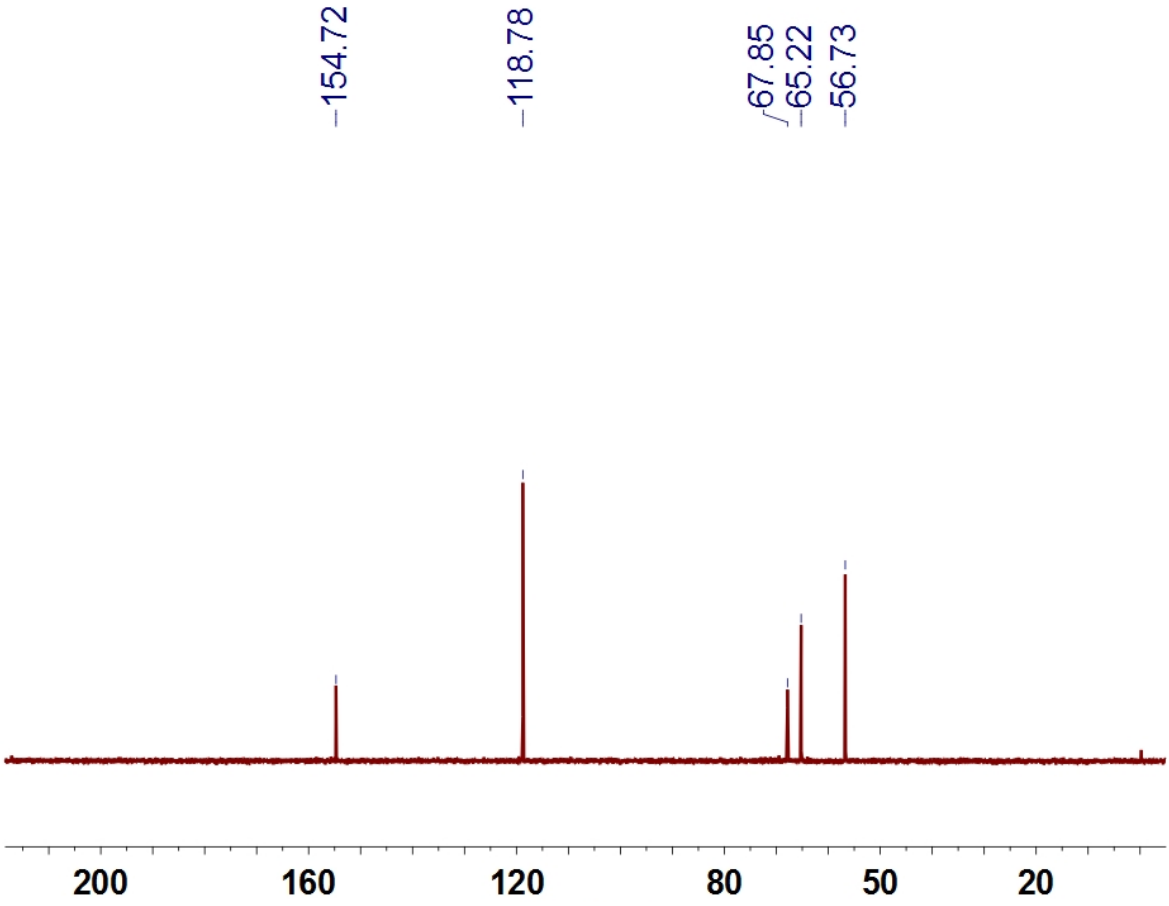

Fig. S2 ^{13}C NMR spectrum (100 MHz, D_2O, 293 K) of **M**.

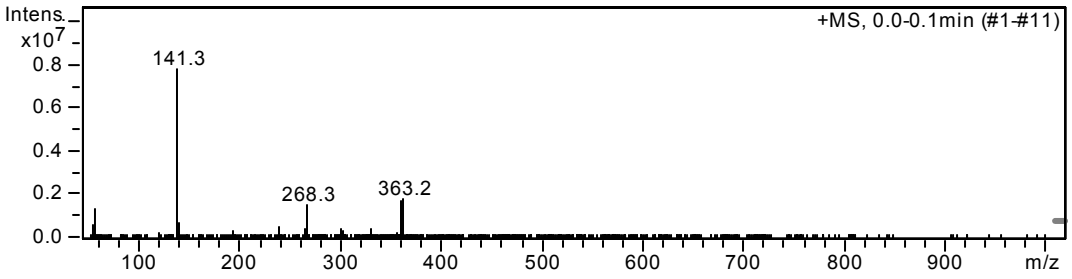

Fig. S3 Electrospray ionization mass spectrum of compound **M**. Assignment of the main peak: *m*/*z* 141.3 $[M - 2Br]^{2+}$.

*3. The investigation of host–guest complexation between **AP5** and **SA** in an aqueous solution at pD 4.0*

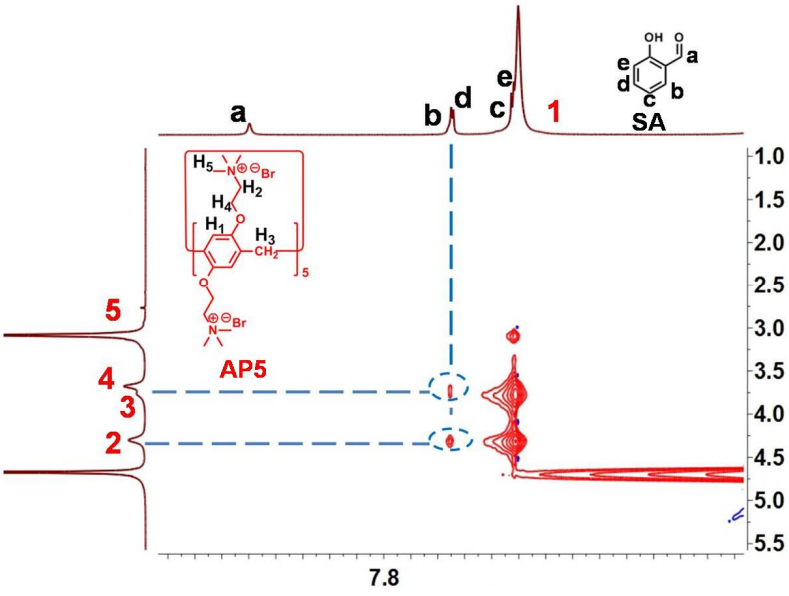

Fig. S4 Partial NOESY NMR spectrum (500 MHz, D_2O, room temperature) of **SA** (10.0 mM) and **AP5** (5.00 mM) at pD 4.0.

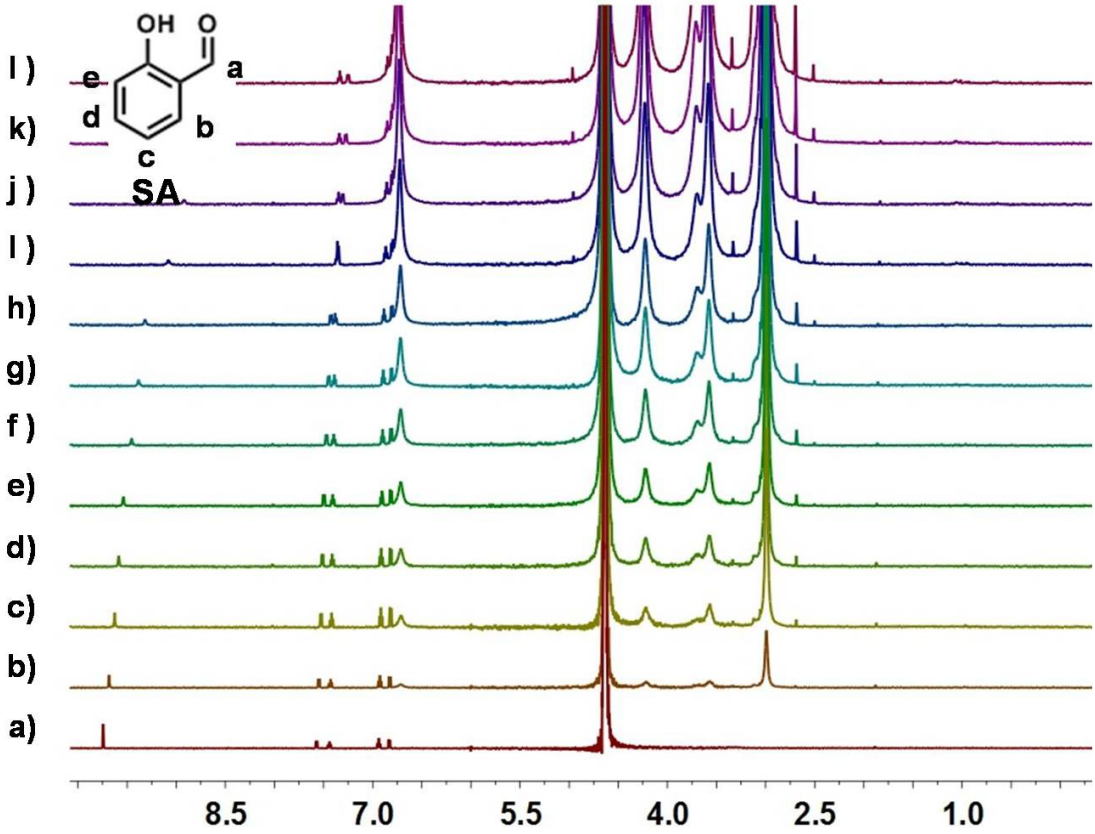

Fig. S5 ^{1}H NMR spectra (D_2O, pD 4.0, 293 K, 400 MHz) of **SA** at a concentration of 1.00 mM with different concentrations of **AP5**: a) 0.000 mM, b) 0.200 mM, c) 0.370 mM, d) 0.520 mM, e) 0.670 mM, f) 0.880 mM, g) 1.20 mM, h) 1.61 mM, i) 3.02 mM, j) 4.61 mM, k) 5.70 mM, and l) 6.67 mM.

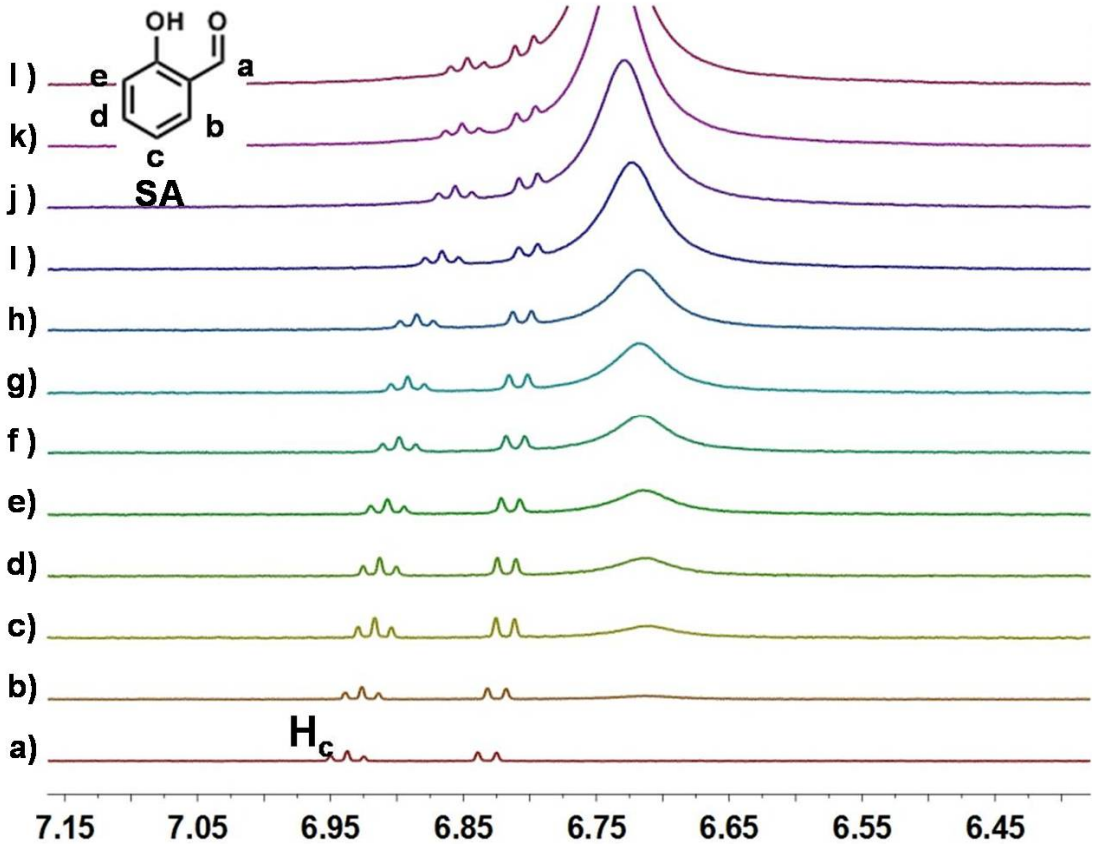

Fig. S6 Partial ^{1}H NMR spectra (D_2O, pD 4.0, 293 K, 400 MHz) of **SA** at a concentration of 1.00 mM with different concentrations of **AP5**: a) 0.000 mM, b) 0.200 mM, c) 0.370 mM, d) 0.520 mM, e) 0.670 mM, f) 0.880 mM, g) 1.20 mM, h) 1.61 mM, i) 3.02 mM, j) 4.61 mM, k) 5.70 mM, and l) 6.67 mM.

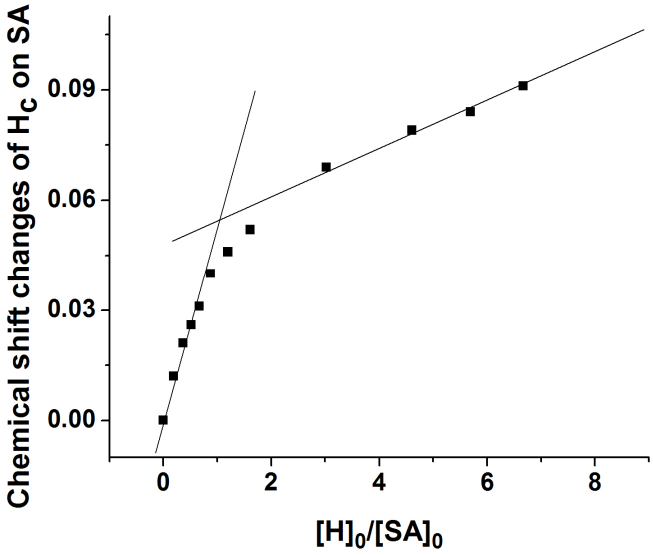

Fig. S7 Mole ratio plot for the complexation between **SA** and **AP5**, indicating a 1:1 stoichiometry.

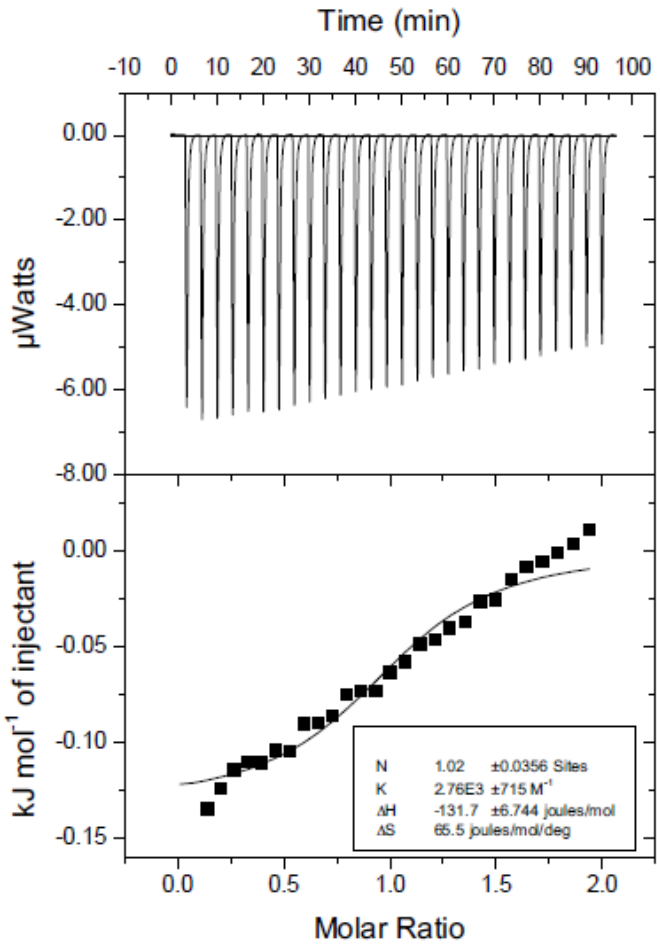

Fig. S8 Microcalorimetric titration of **AP5** with **SA** in aqueous solution (pH 4) at 303.15 K. Top: Raw ITC data for 26 sequential injections (10 µL per injection) of a **SA** solution (20.0 mM) into an **AP5** solution (1.00 mM). Bottom: Net reaction heat obtained from the integration of the calorimetric traces.

*4. The investigation of host–guest complexation between **AP5** and **SA**⁻ in an aqueous solution at pD 11.0*

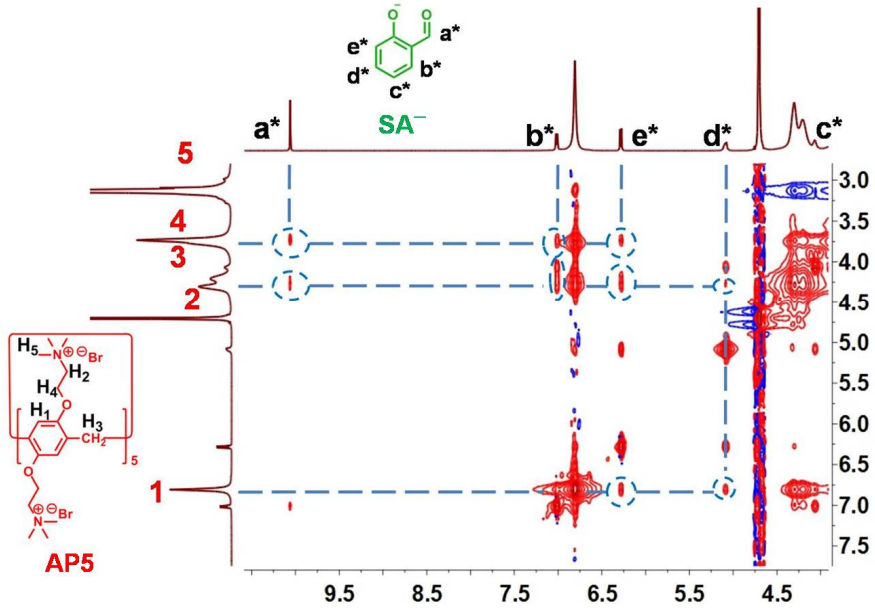

Fig. S9 Partial NOESY NMR spectrum (500 MHz, D_2O, room temperature) of **SA**⁻ (5.00 mM) and **AP5** (5.00 mM) at pD 11.0.

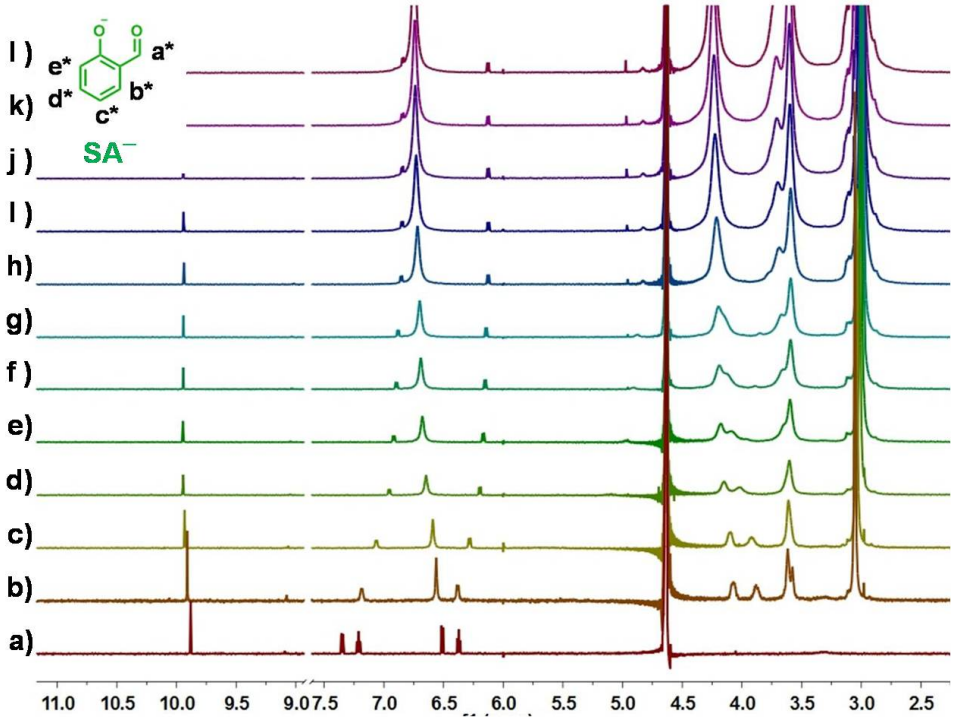

Fig. S10 ^{1}H NMR spectra (D_2O, pD 11.0, 293 K, 400 MHz) of **SA**⁻ at a concentration of 1.00 mM with different concentrations of **AP5**: a) 0.000 mM, b) 0.310 mM, c) 0.550 mM, d) 0.810 mM, e) 1.01 mM, f) 1.40 mM, g) 1.60 mM, h) 3.22 mM, i) 4.22 mM, j) 4.90 mM, k) 6.02 mM, and l) 6.80 mM.

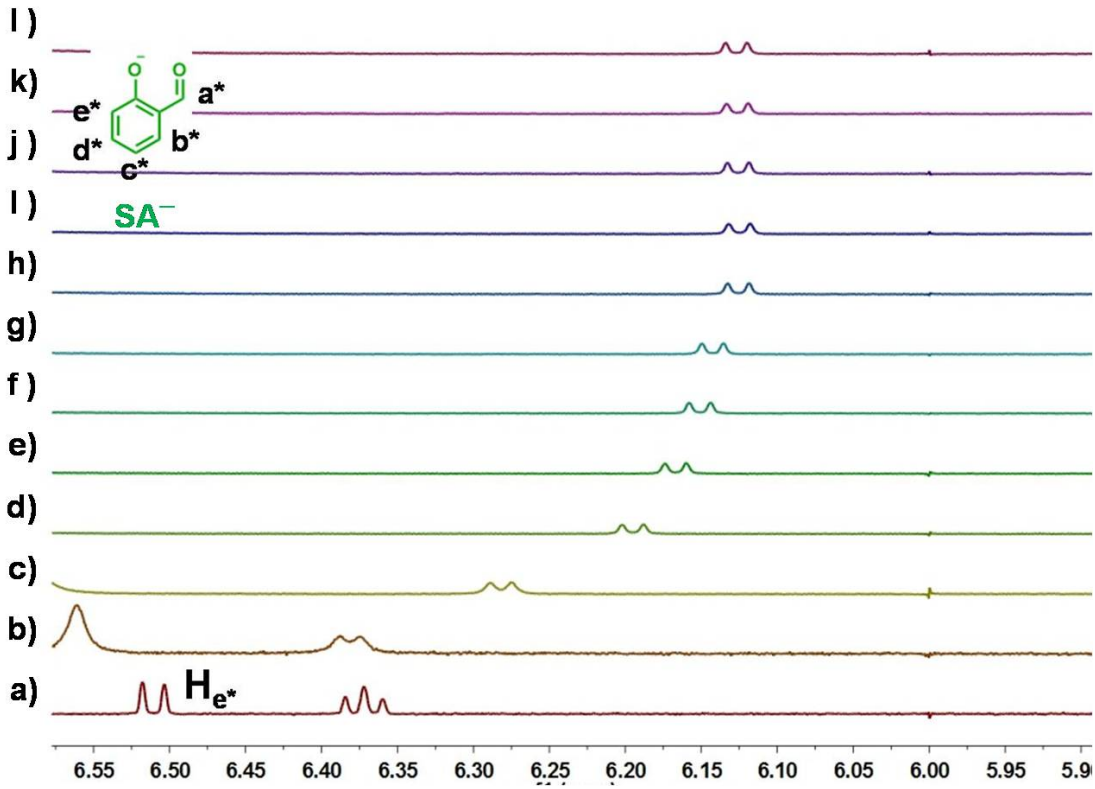

Fig. S11 Partial ^{1}H NMR spectra (D_2O, pD 11.0, 293 K, 400 MHz) of **SA** at a concentration of 1.00 mM with different concentrations of **AP5**: a) 0.000 mM, b) 0.310 mM, c) 0.550 mM, d) 0.810 mM, e) 1.01 mM, f) 1.40 mM, g) 1.60 mM, h) 3.22 mM, i) 4.22 mM, j) 4.90 mM, k) 6.02 mM, and l) 6.80 mM.

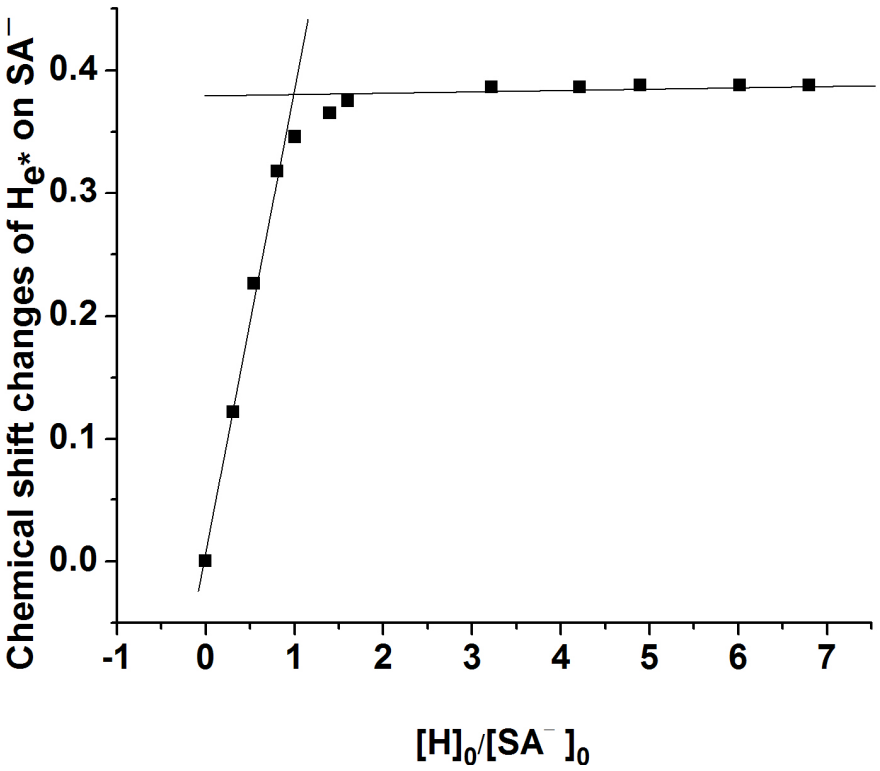

Fig. S12 Mole ratio plot for the complexation between **SA**$^-$ and **AP5**, indicating a 1:1 stoichiometry.

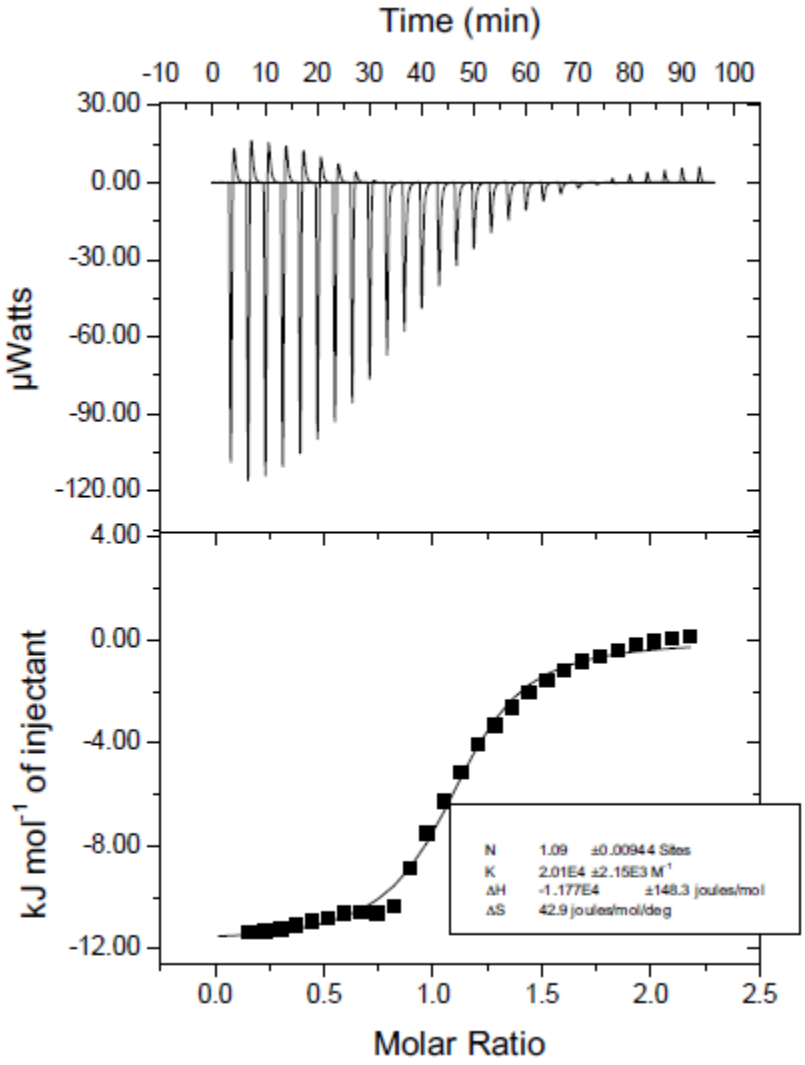

Fig. S13 Microcalorimetric titration of **AP5** with **SA**$^{-}$ in aqueous solution (pH 11) at 303.15 K. Top: Raw ITC data for 26 sequential injections (10 µL per injection) of a **SA**$^{-}$ solution (20.0 mM) into an **AP5** solution (1.00 mM). Bottom: Net reaction heat obtained from the integration of the calorimetric traces.

*5. Fluorescence intensity of salicylaldehyde in the absence and presence of **AP5** at different pH values*

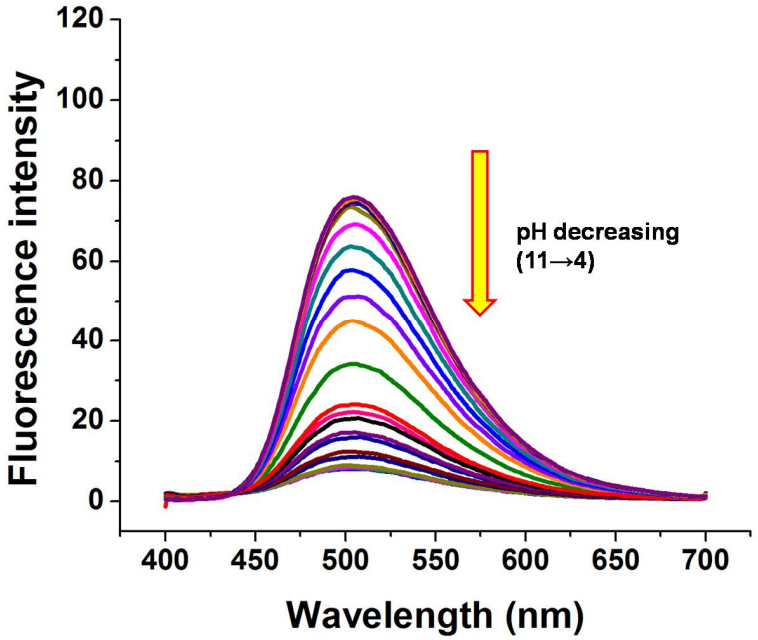

Fig. S14 Fluorescence titration of a solution of salicylaldehyde (5.00×10^{-4} M, λ_{ex} = 370 nm, λ_{em} = 502 nm) upon lowering pH in water.

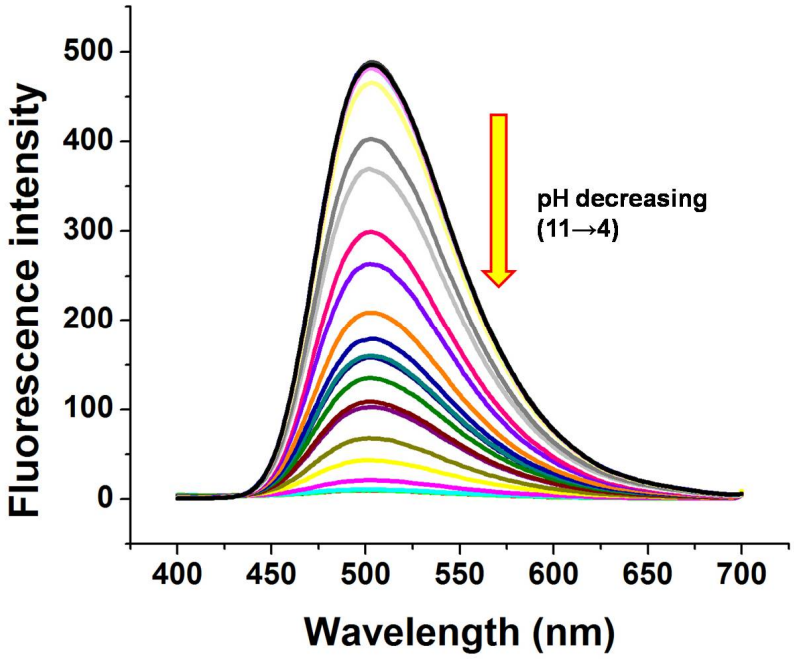

Fig. S15 Fluorescence titration of a 2:1 mixture of **AP5** and salicylaldehyde upon lowering pH in water (5.00×10^{-4} M salicylaldehyde, λ_{ex} = 370 nm, λ_{em} = 502 nm).

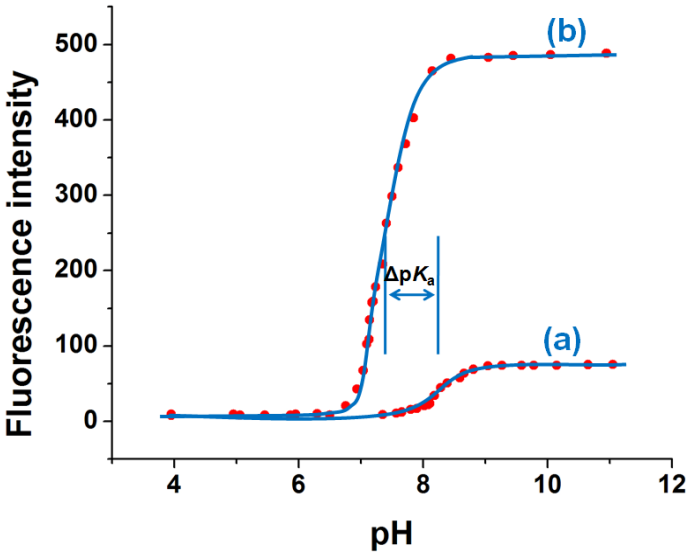

Fig. S16 Fluorescence intensity of salicylaldehyde in the absence (a) and presence (b) of 2 equiv. of **AP5** at different pH values (5.00×10^{-4} M salicylaldehyde, λ_{ex} = 370 nm, λ_{em} = 502 nm). The pH value of the solution was adjusted by adding HCl or NaOH.

*6. The four-state model explaining the prototropic equilibrium between **SA** and **SA**$^-$ in the absence and presence of **AP5**.*

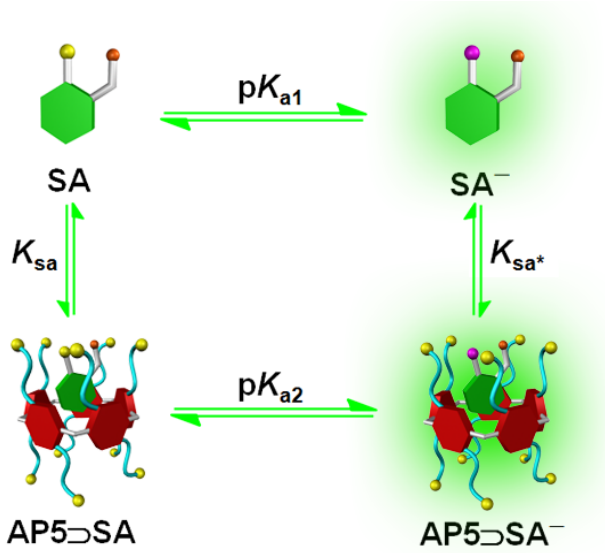

$$K_{a2} = K_{a1} \times K_{sa*} / K_{sa} \qquad \textbf{(S1)}$$

Scheme S2. The four-state model explaining the prototropic equilibrium between **SA** and **SA**$^-$ in the absence and presence of **AP5**.

*7. Association constant determination for **AP5**⊃salicylaldehyde in PBS at pH 7.2*

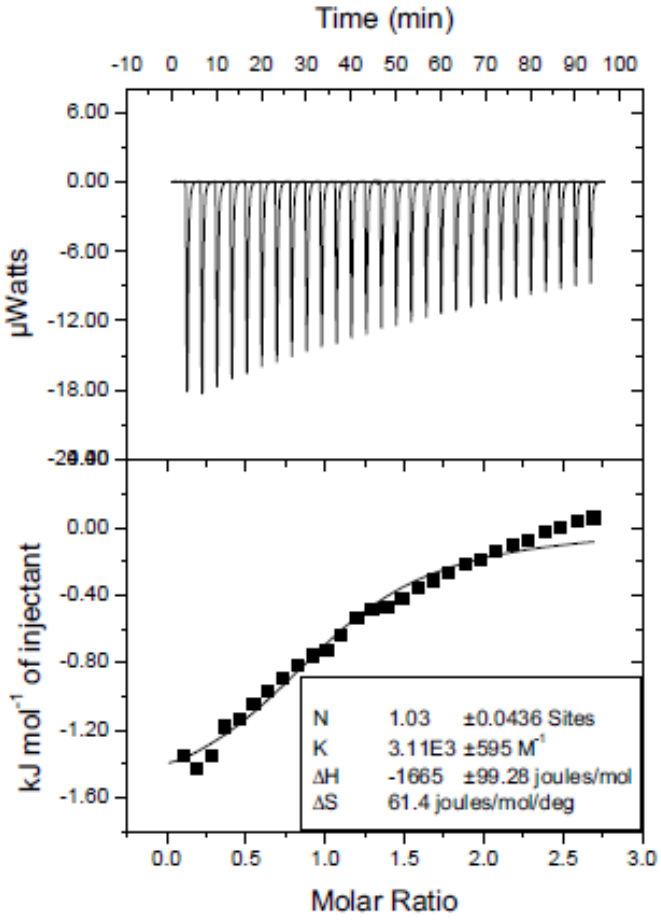

Fig. S17 Microcalorimetric titration of **AP5** with salicylaldehyde in PBS (pH 7.2) at 303.15 K. (Top) Raw ITC data for 26 sequential injections (10 µL per injection) of a salicylaldehyde-containing solution (20.0 mM) into an **AP5** solution (1.00 mM). (Bottom) Net reaction heat obtained from the integration of the calorimetric traces.

*8. The investigation of host–guest complexation between **AP5** and phenolic compounds **G1–G6***

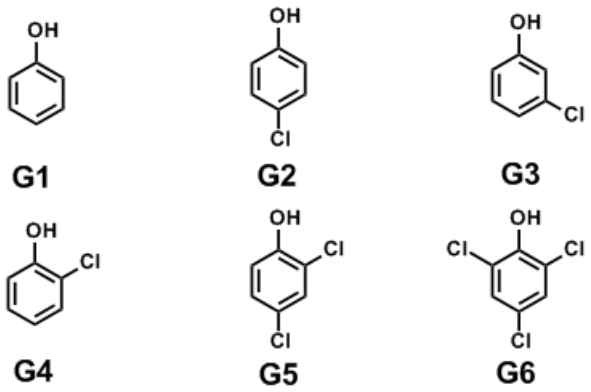

Fig. S18 Chemical structure of phenolic compounds used here.

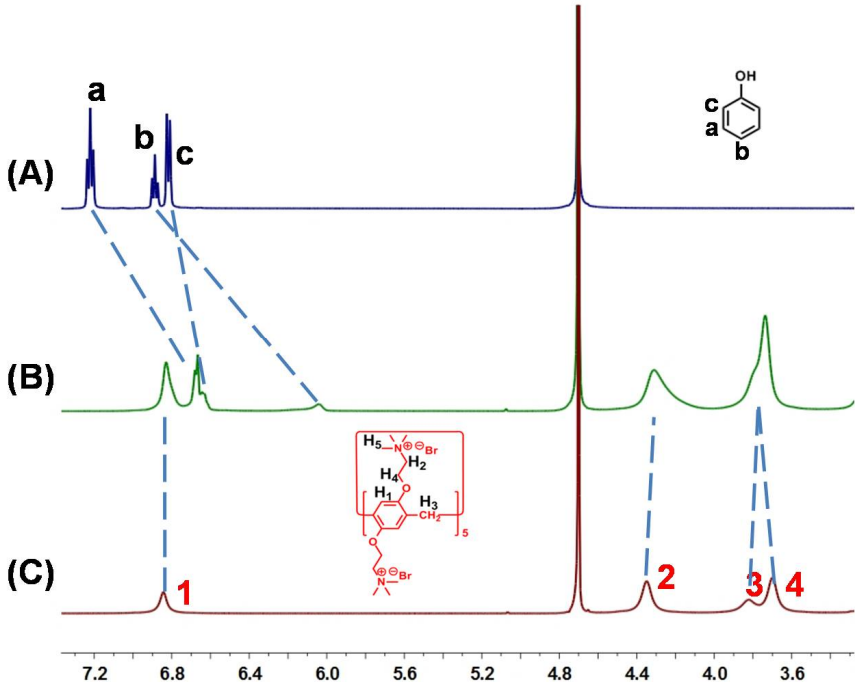

Fig. S19 ^{1}H NMR spectra (400 MHz, D_2O, 293 K): (A) **G1** (4.00 mM); (B) **G1** (4.00 mM) and **AP5** (2.00 mM); (C) **AP5** (2.00 mM).

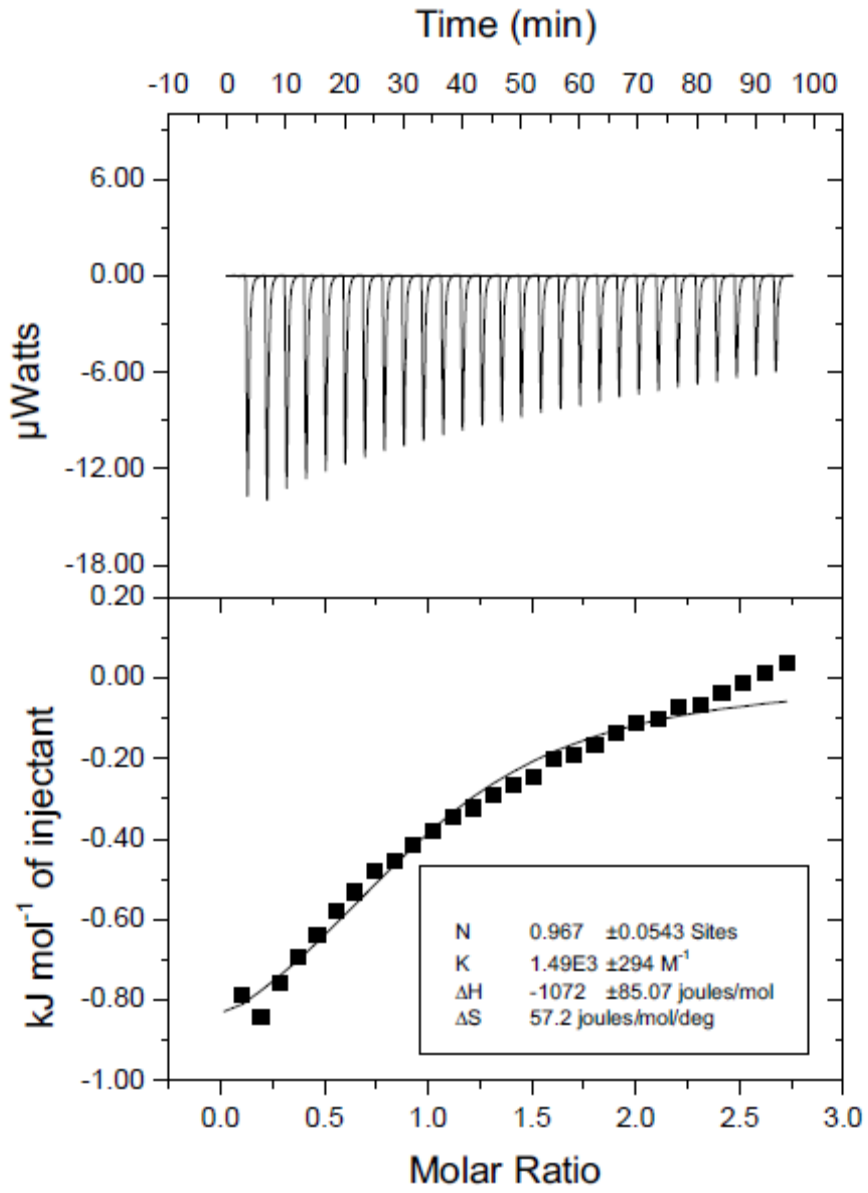

Fig. S20 Microcalorimetric titration of **AP5** with **G1** in PBS (pH 7.2) at 303.15 K. Top: Raw ITC data for 26 sequential injections (10 µL per injection) of a **G1** solution (20.0 mM) into an **AP5** solution (1.00 mM). Bottom: Net reaction heat obtained from the integration of the calorimetric traces.

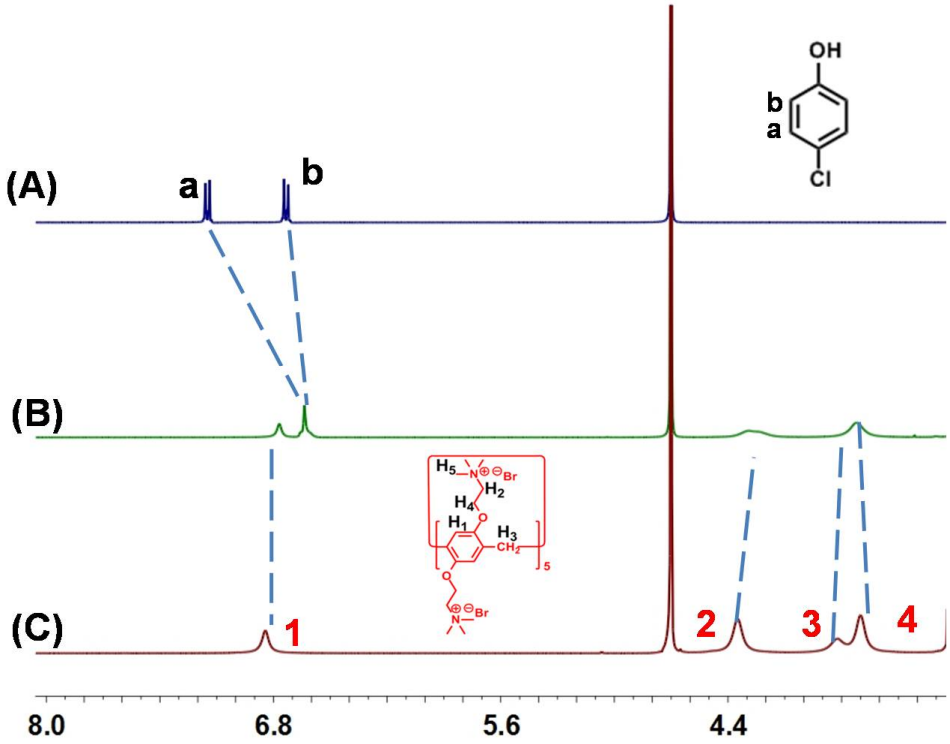

Fig. S21 ^{1}H NMR spectra (400 MHz, D_2O, 293 K): (A) **G2** (4.00 mM); (B) **G2** (4.00 mM) and **AP5** (2.00 mM); (C) **AP5** (2.00 mM).

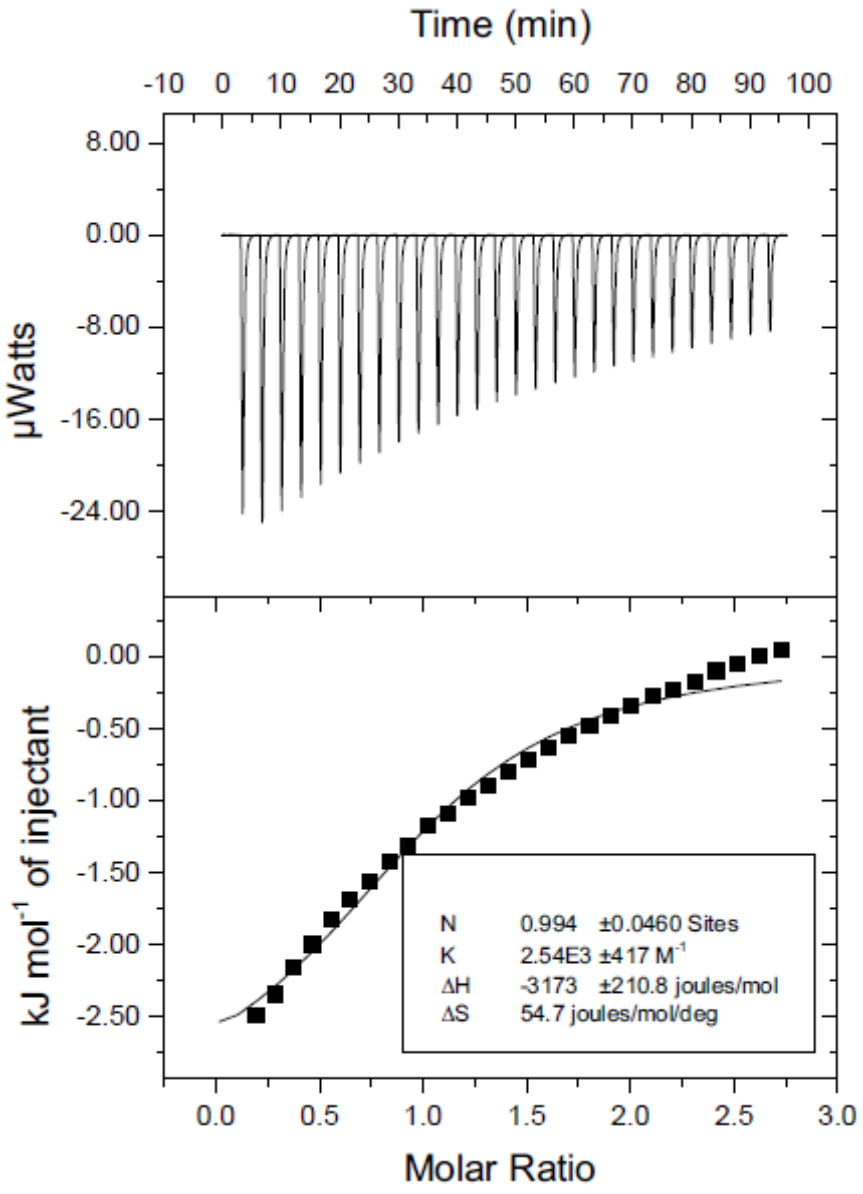

Fig. S22 Microcalorimetric titration of **AP5** with **G2** in PBS (pH 7.2) at 303.15 K. Top: Raw ITC data for 26 sequential injections (10 µL per injection) of a **G2** solution (20.0 mM) into an **AP5** solution (1.00 mM). Bottom: Net reaction heat obtained from the integration of the calorimetric traces.

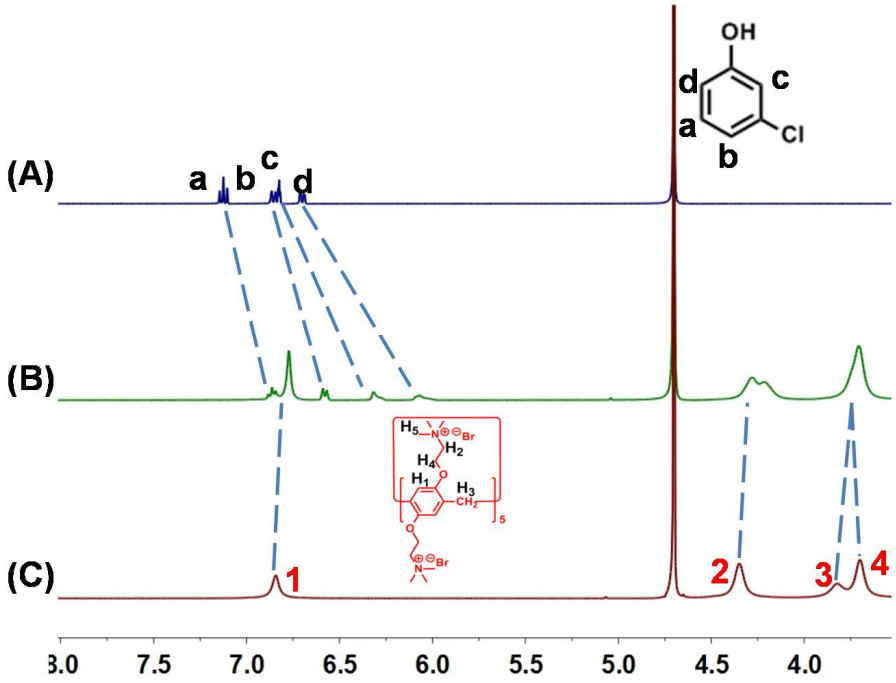

Fig. S23 ^{1}H NMR spectra (400 MHz, D_2O, 293 K): (A) **G3** (4.00 mM); (B) **G3** (4.00 mM) and **AP5** (2.00 mM); (C) **AP5** (2.00 mM).

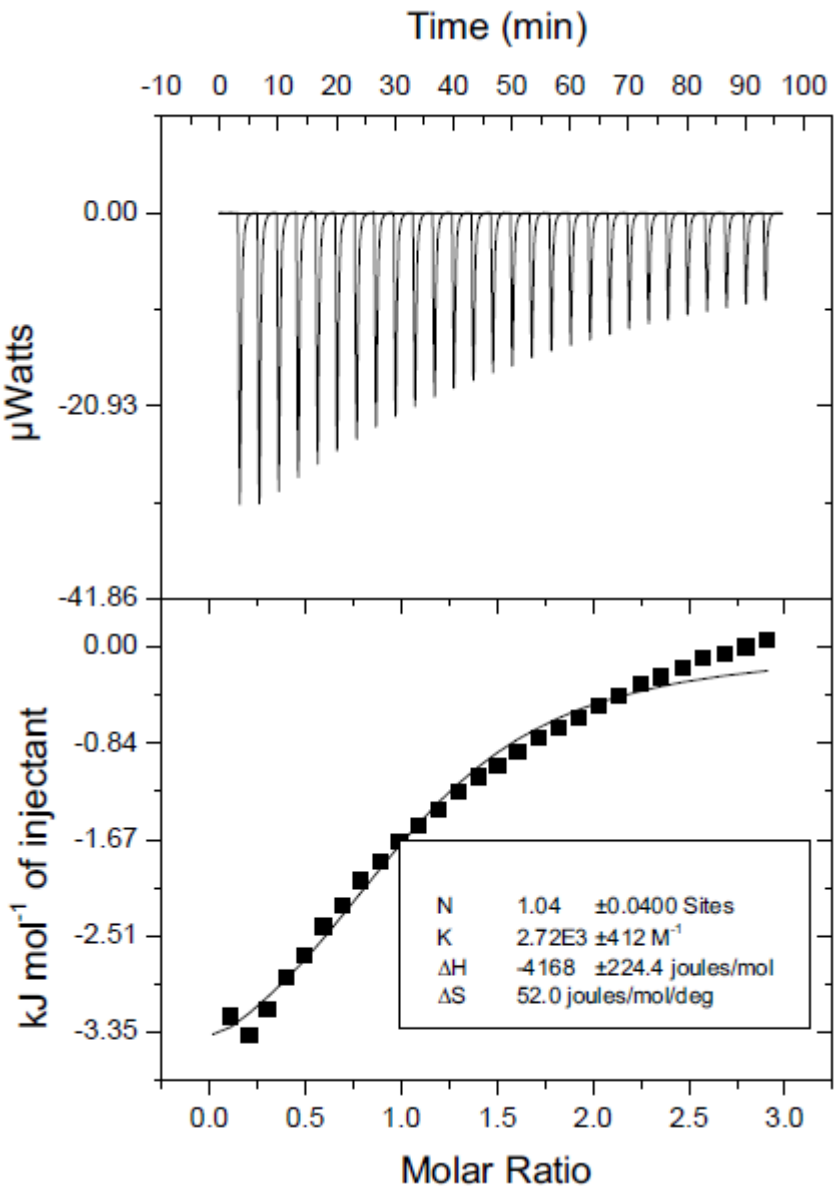

Fig. S24 Microcalorimetric titration of **AP5** with **G3** in PBS (pH 7.2) at 303.15 K. Top: Raw ITC data for 26 sequential injections (10 µL per injection) of a **G3** solution (20.0 mM) into an **AP5** solution (1.00 mM). Bottom: Net reaction heat obtained from the integration of the calorimetric traces.

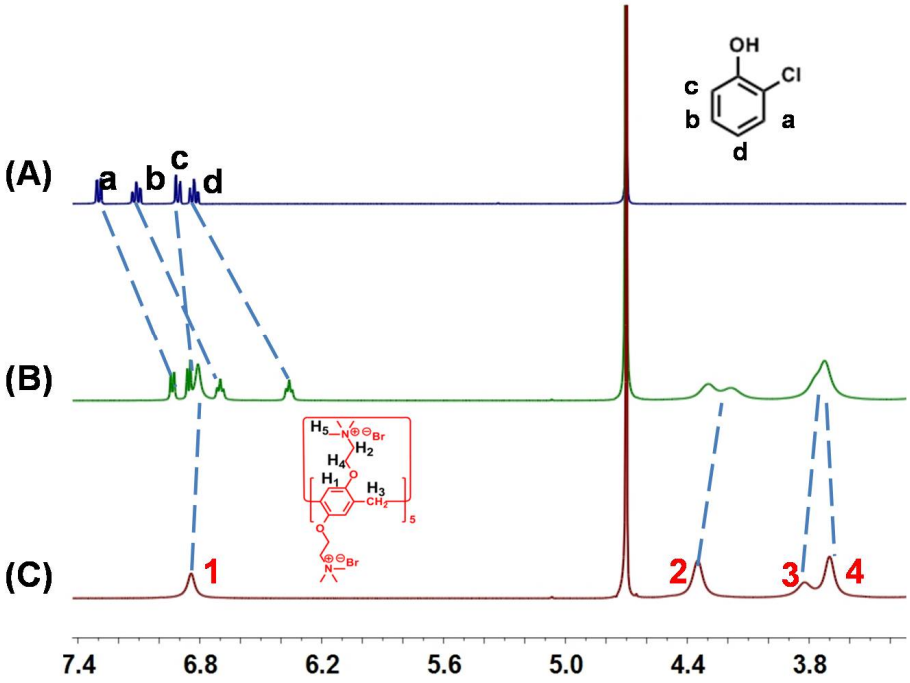

Fig. S25 ^{1}H NMR spectra (400 MHz, D_2O, 293 K): (A) **G4** (4.00 mM); (B) **G4** (4.00 mM) and **AP5** (2.00 mM); (C) **AP5** (2.00 mM).

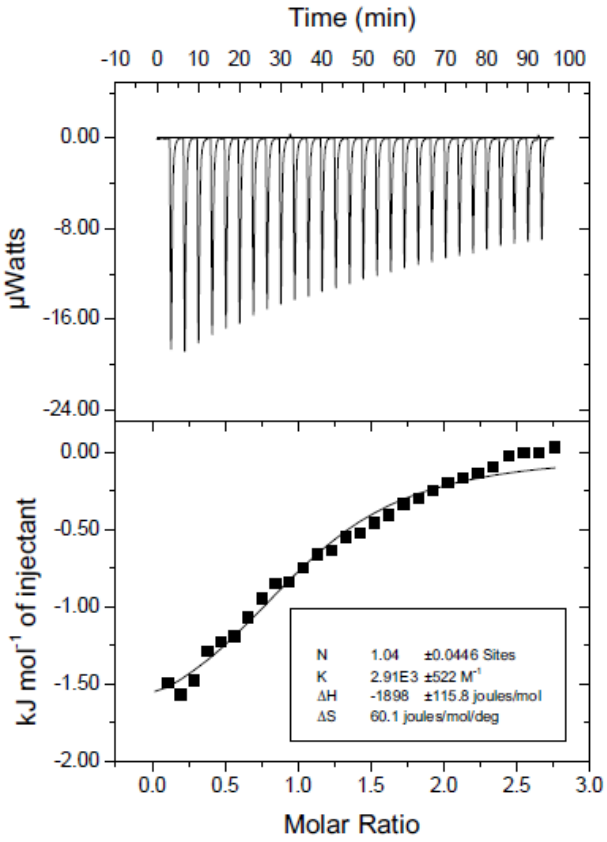

Fig. S26 Microcalorimetric titration of **AP5** with **G4** in PBS (pH 7.2) at 303.15 K. Top: Raw ITC data for 26 sequential injections (10 µL per injection) of a **G4** solution (20.0 mM) into an **AP5** solution (1.00 mM). Bottom: Net reaction heat obtained from the integration of the calorimetric traces.

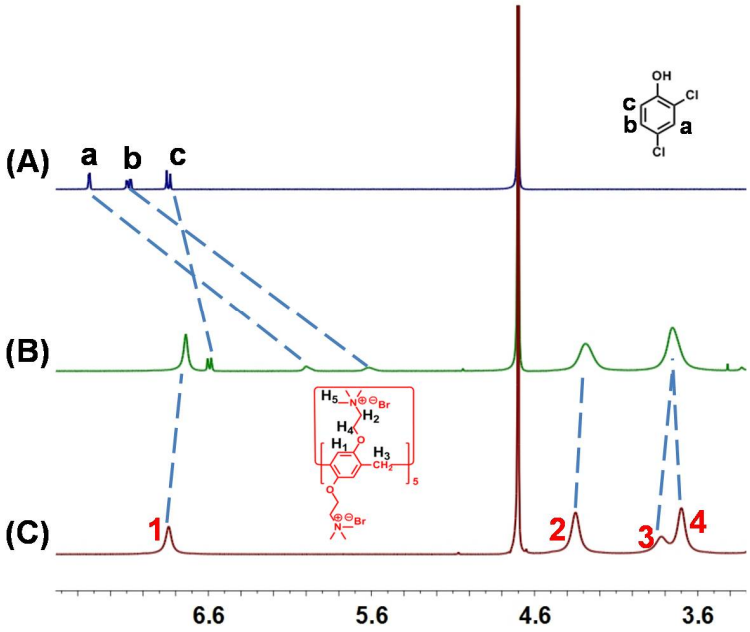

Fig. S27 ^{1}H NMR spectra (400 MHz, D_2O, 293 K): (A) **G5** (4.00 mM); (B) **G5** (4.00 mM) and **AP5** (2.00 mM); (C) **AP5** (2.00 mM).

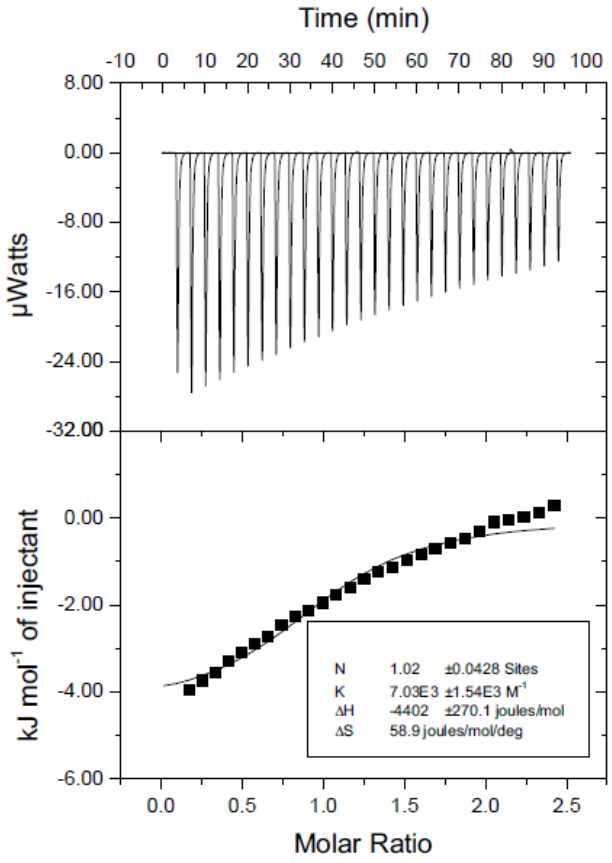

Fig. S28 Microcalorimetric titration of **AP5** with **G5** in PBS (pH 7.2) at 303.15 K. Top: Raw ITC data for 26 sequential injections (10 μL per injection) of a **G5** solution (20.0 mM) into an **AP5** solution (1.00 mM). Bottom: Net reaction heat obtained from the integration of the calorimetric traces.

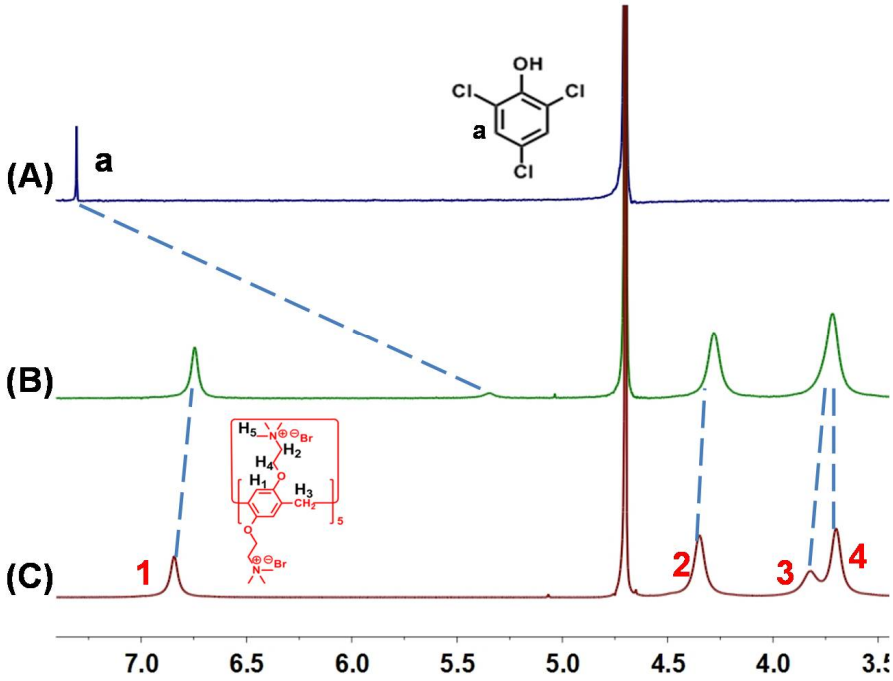

Fig. S29 ^{1}H NMR spectra (400 MHz, D_2O, 293 K): (a) **G6** (2.00 mM); (b) **G6** (2.00 mM) and **AP5** (2.00 mM); (c) **AP5** (2.00 mM).

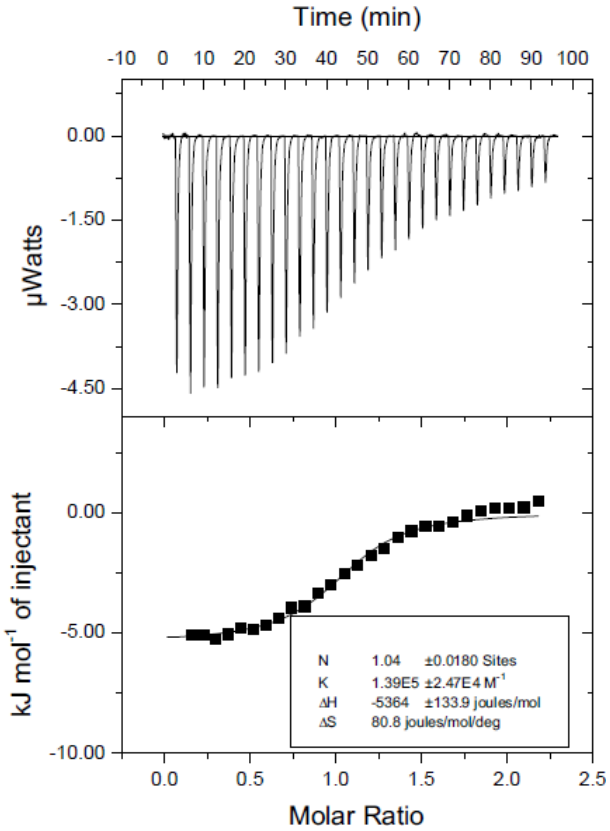

Fig. S30 Microcalorimetric titration of **AP5** with **G6** in PBS (pH 7.2) at 303.15 K. Top: Raw ITC data for 26 sequential injections (10 µL per injection) of a **G6** solution (20.0 mM) into an **AP5** solution (1.00 mM). Bottom: Net reaction heat obtained from the integration of the calorimetric traces.

*9. Fluorescence titration for the competitive displacement of salicylaldehyde from **AP5** by various phenolic compounds in PBS at pH 7.2*

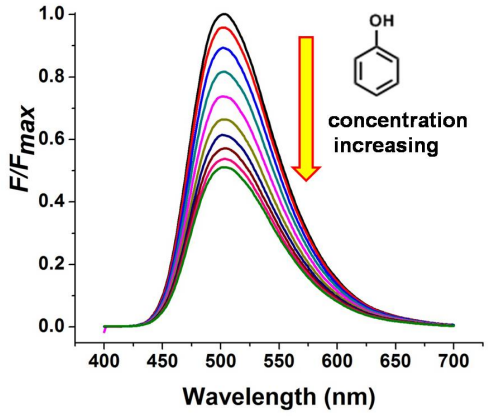

Fig. S31 Fluorescence titration for the competitive displacement of salicylaldehyde (0.500 mM) from **AP5** (1.00 mM) by **G1** (0, 0.250, 0.750, 1.50, 2.50, 3.75, 5.00, 6.25, 7.50, and 8.75 mM) in PBS at pH 7.2 (λ_{ex} = 370 nm, λ_{em} = 502 nm).

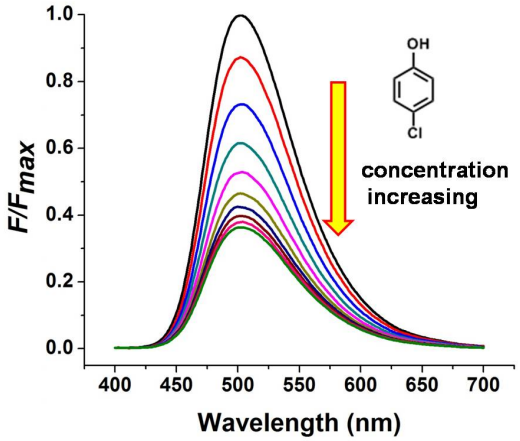

Fig. S32 Fluorescence titration for the competitive displacement of salicylaldehyde (0.500 mM) from **AP5** (1.00 mM) by **G2** (0, 0.250, 0.750, 1.50, 2.50, 3.75, 5.00, 6.25, 7.50, and 8.75 mM) in PBS at pH 7.2 (λ_{ex} = 370 nm, λ_{em} = 502 nm).

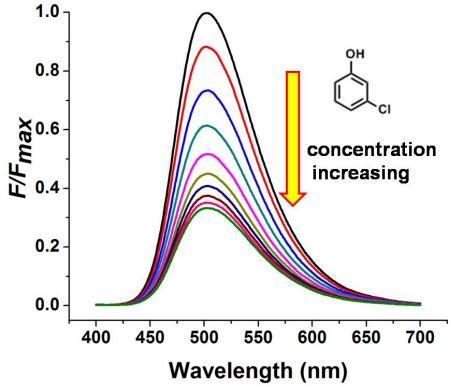

Fig. S33 Fluorescence titration for the competitive displacement of salicylaldehyde (0.500 mM) from **AP5** (1.00 mM) by **G3** (0, 0.250, 0.750, 1.50, 2.50, 3.75, 5.00, 6.25, 7.50, and 8.75 mM) in PBS at pH 7.2 (λ_{ex} = 370 nm, λ_{em} = 502 nm).

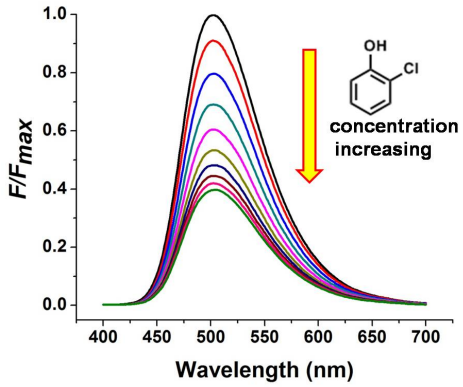

Fig. S34 Fluorescence titration for the competitive displacement of salicylaldehyde (0.500 mM) from **AP5** (1.00 mM) by **G4** (0, 0.250, 0.750, 1.50, 2.50, 3.75, 5.00, 6.25, 7.50, 8.75 and mM) in PBS at pH 7.2 (λ_{ex} = 370 nm, λ_{em} = 502 nm).

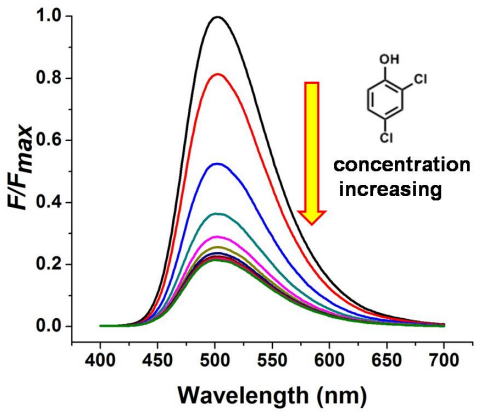

Fig. S35 Fluorescence titration for the competitive displacement of salicylaldehyde (0.500 mM) from **AP5** (1.00 mM) by **G5** (0, 0.250, 0.750, 1.50, 2.50, 3.75, 5.00, 6.25, 7.50, and 8.75 mM) in PBS at pH 7.2 (λ_{ex} = 370 nm, λ_{em} = 502 nm).

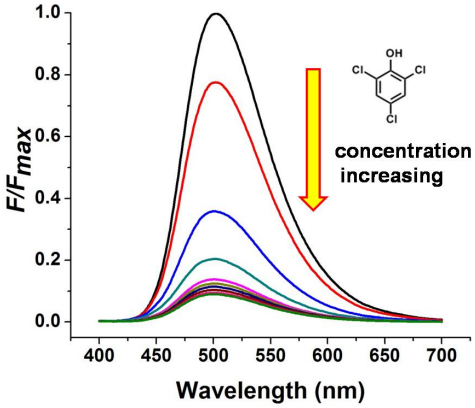

Fig. S36 Fluorescence titration for the competitive displacement of salicylaldehyde (0.500 mM) from **AP5** (1.00 mM) by **G6** (0, 0.250, 0.750, 1.50, 2.50, 3.75, 5.00, 6.25, 7.50, and 8.75 mM) in PBS at pH 7.2 (λ_{ex} = 370 nm, λ_{em} = 502 nm).

*10. The solution colors of salicylaldehyde in the absence and presence of **AP5***

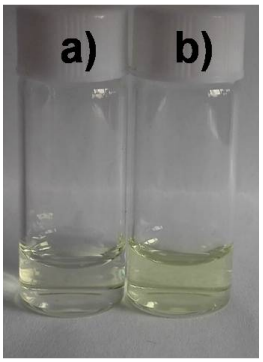

Fig. S37 The solution colors of 0.500 mM salicylaldehyde in the absence a) and presence b) of 3.50 mM **AP5**.

11. Reference

S1. Y. Ma, X. Ji, F. Xiang, X. Chi, C. Han, J. He, Z. Abliz, W. Chen and Huang, F. *Chem. Commun.* 2011, **47**, 12340–12342.